The stress-strain state simulation for the auger-boring machine's support-guide system

Aleksei Khoreshok[1], *Leonid* Mametyev[1], *Oleg* Lyubimov[2*], *Andrey* Kuznetsov[3], and *Yunliang* Tan[4]

[1]T.F. Gorbachev Kuzbass State Technical University, Department of Mining Machines and Complexes, 650000 Kemerovo, 28 Vesennyaya st., Russian Federation
[2]T.F. Gorbachev Kuzbass State Technical University, Department of Information and Automated Production Systems, 650000 Kemerovo, 28 Vesennyaya st., Russian Federation
[3]T.F. Gorbachev Kuzbass State Technical University, Prokopyevsk branch, Department of Information Technologies, Mechanical Engineering and Motor Transport, 653033 Prokopyevsk, 19 Nogradskaya st., Russian Federation
[4] State Key Laboratory of Mining Disaster Prevention and Control Co-founded by Shandong Province and the Ministry of Science and Technology, Qingdao 266590, China

Abstract. The article deals with a number of important aspects of the aggregate-modular type auger-boring equipment creation, as an integral part of the range of tunneling complexes for mining operations and laying horizontal and slightly deviated holes for various purposes. The importance of improving the support and guide systems, characterized by a variety of configurations and sizes, a large number of elements for various purposes and with different responsibility degree, is noted separately. In this regard, the possibility of flexible refinement of the complexes configuration for specific boring conditions with the verification of each applied technical solution by computer modeling remains relevant. The ways for a new constructive solutions creating are outlined.

1 Introduction

In the Siberian region, as well as in Russia and in the world as a whole, an active scientific and applied works is being carried out currently. The result of this work is the tunneling complexes implementation for a wide range of purposes, intended for mining and laying horizontal and slightly deviated holes for various purposes [1-12].

In the Kuzbass State Technical University (KuzSTU), the Department of Mining Machines and Complexes and the Department of Information and Automated Production Systems, with the involvement of interested specialists, a range of auger-boring complexes for horizontal boring built on the aggregate-modular principle are developing. At the same time, it is taken into account that in order to increase the stability of boring equipment when boring horizontal holes of large diameter, it is possible to use a two-stage technology, which implies boring a small-diameter pioneer hole in a direct motion with its subsequent boring to the required diameter in a reverse motion. It is recommended, to implement this, to

---

combine the projection of the hole's boring axis with the axial forces transmission plane's of boring machine feeding mechanism [13-15]. After a pilot industrial operation of complexes for trenchless laying of communications, presented by a number of developers, including KuzSTU, it was found that the supply of the machine unit into and out from the mine face at horizontal boring process can be successfully carried out cyclically, if the following problems will overcome [16-18]:

- the complexity of ensuring the stepping nature of the translational action hydraulic engines operation;
- high bending moment on the casing pipe due to the stops location is outside the hole's boring axis;
- difficult automation of the process.

The implementation of technical solutions in the design of auger-boring complexes that allow to overcome the above-mentioned problems is possible when modeling the working state of the support and guide systems, characterized by a variety of configurations and sizes, a large number of elements for various purposes and responsibility degree.

In the design of the auger-boring equipment considered in this work, the operability of the cyclic feeding mechanisms completely depends on the strength indicators of the support-guide system (fig.1, 2), the geometric characteristics of the cut-sections and on the physical and mechanical properties of its parts materials.
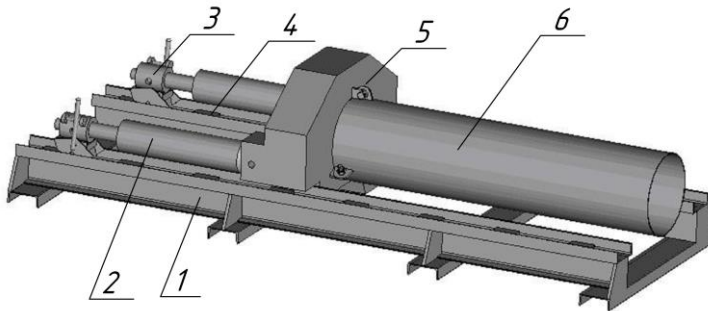

Fig. 1. General view of the auger-boring machine's support-guide system in the initial position: 1-modular multipart frame; 2-hydraulic jack; 3-movable thrust shoes; 4-fixed stops of the modular frame; 5 - power frontal part of the running carriage; 6- casing pipe's sectional column.
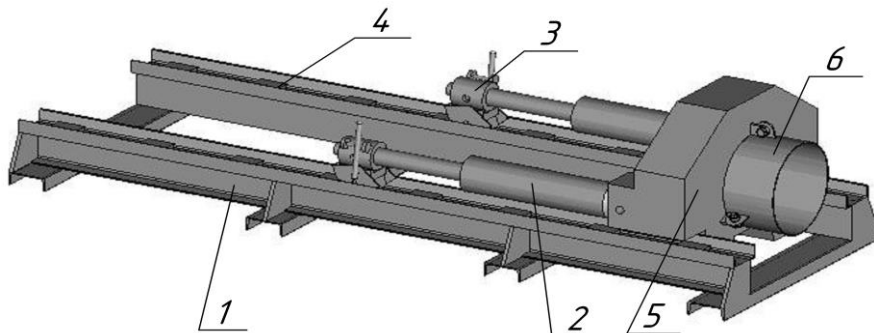

Fig. 2. General view of the auger-boring machine's support-guide system in the final position: 1-modular multipart frame; 2-hydraulic jack; 3-movable thrust shoes; 4-fixed stops of the modular frame; 5 - power frontal part of the running carriage; 6- casing pipe's sectional column.

In connection with the above, it is very relevant to quickly assess the stress-strain state of the support and guide system of the auger-boring machine in conditions of various external loading, its working position, the design of the frontal part, various casing pipe's diameters and the length of the hydraulic jack rod overhang.

2 Materials and methods

To identify recommendations for improving the design of the support-guide system design improving, it is necessary to simulate its stress-strain state both in the initial position of a horizontal hole boring, where the casing pipe has a maximum length, with a variable hydraulic cylinder rod's overhang, and in the final position, at the end of boring, where the length of the casing pipe is minimal.

The changes in the stress-strain state of the support-guide system structure with variation in the hydraulic cylinder force from 10 to 40 tons was studied. In the course of the research, stress concentration zones were identified. Figures 3 and 4 shows the results of the support-guide system state modeling in the initial position with the minimum and maximum hydraulic cylinder rod's overhang.
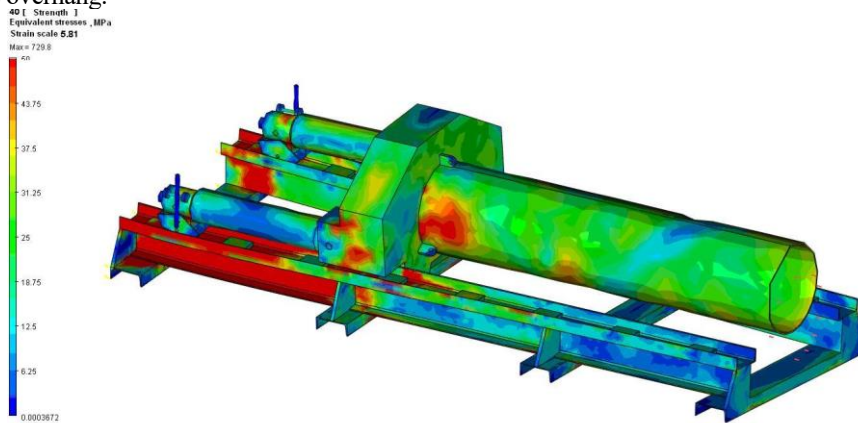

Fig. 3. The support-guide system's stress-strain state in the initial position with the minimum hydraulic cylinder rod's overhang
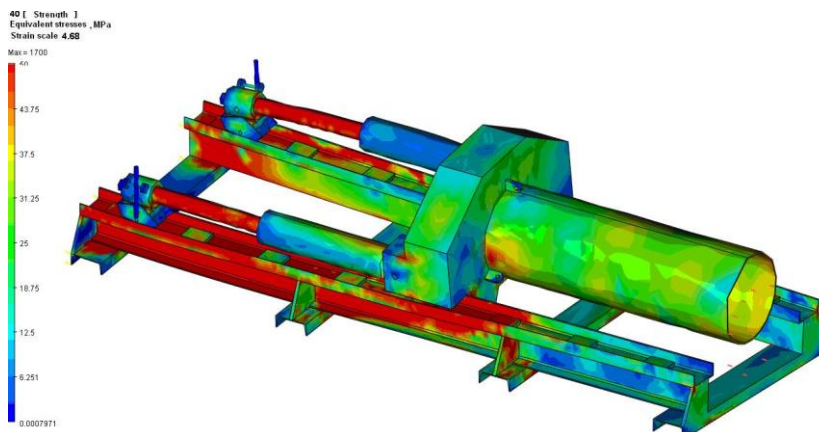
Fig. 4. The support-guide system's stress-strain state in the initial position with the maximum hydraulic cylinder rod's overhang

Figures 5 and 6 shows the results of modeling the support-guide system state in the final position with the minimum and maximum overhang of the hydraulic cylinder rod.
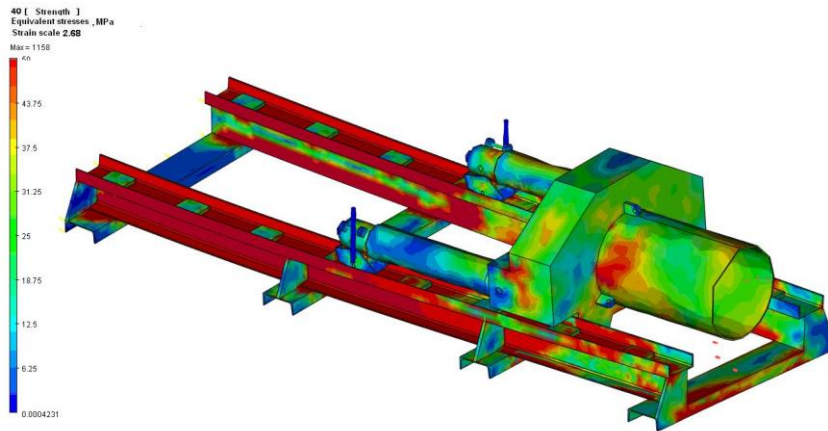

Fig. 5. The support-guide system's stress-strain state in the final position with the minimum hydraulic cylinder rod's overhang
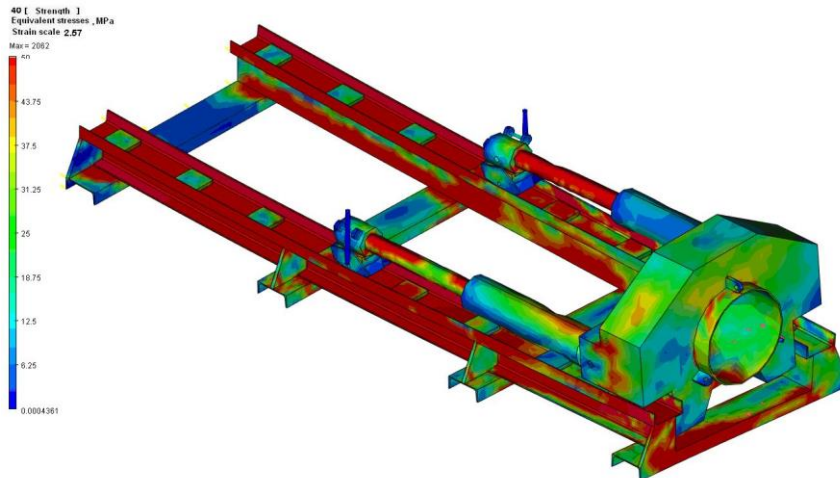

Fig. 6. The support-guide system's stress-strain state in the final position with the maximum hydraulic cylinder rod's overhang

As can be seen from the illustrations, the simulation results are very pictorial, allowed for detalization and, definitely, are easily interpreted, which is confirmed by the data below.

3 Результаты и обсуждение

Based on the results of the support-guide system state modeling in the initial and final positions, with different forces on the hydraulic cylinder from 10 to 40 tons, the dependences of the stress and deformation of the hydraulic cylinder rod and the frontal's hinge on the rod's overhang in the initial and final positions are revealed.

Table 1 shows the polynomial dependences of the stresses in the rod on its overhang and the applied force. The graph of the dependence of the stresses in the rod on its overhang in the initial position at different forces is shown in fig. 7.

Table 1. Polynomial dependences of the stresses in the rod on its overhang and the applied force

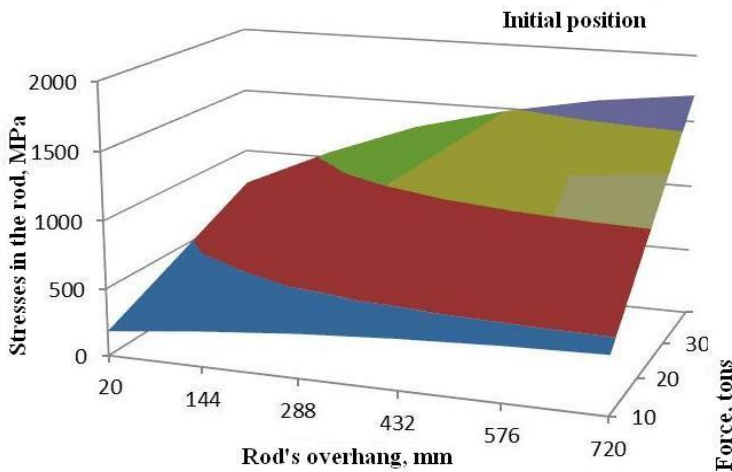| Force, tons	Polynoms	R^2
10	$y = -0.0004x^2 + 0.6364x + 173.31$	0.9988
20	$y = -0.0008x^2 + 1.2809x + 345.55$	0.9988
30	$y = -0.0012x^2 + 1.9204x + 518.42$	0.9988
40	$y = -0.0016x^2 + 2.5551x + 691.59$	0.9987

Fig. 7. The graph of the dependence of the stresses in the rod on its overhang in the initial position

Table 2 shows the polynomial dependences of the stresses in the rod on its overhang and the applied force. The graph of the dependence of the stresses in the rod on its overhang in the final position is shown in fig. 8.

Table 2. Polynomial dependences of the stresses in the rod on its overhang and the applied force

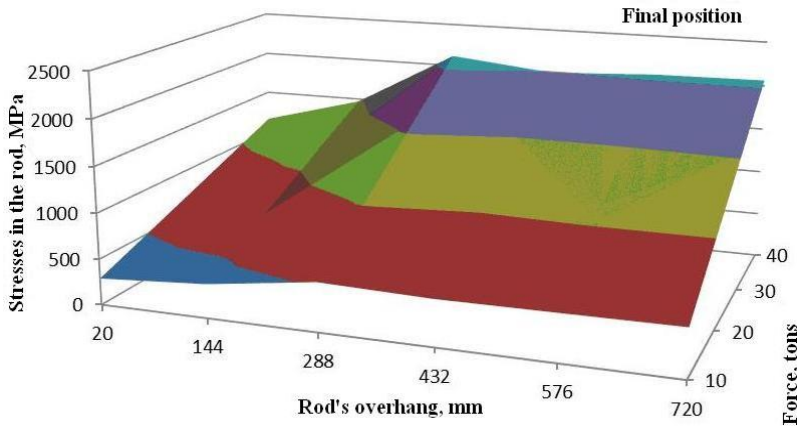| Force, tons	Polynoms	R^2
10	$y = 1E\text{-}06x^3 - 0.0025x^2 + 1.4222x + 249.61$	0.9211
20	$y = 2E\text{-}06x^3 - 0.0046x^2 + 2.7402x + 502.67$	0.9241
30	$y = 5E\text{-}06x^3 - 0.0078x^2 + 4.3423x + 746.26$	0.9193
40	$y = 5E\text{-}06x^3 - 0.0093x^2 + 5.5289x + 1003.5$	0.9236

Fig. 8. The graph of the dependence of the stresses in the rod on its overhang in the final position

Table 3 shows the polynomial dependences of the deformations of the rod on its overhang and the applied force. The graph of the dependence of the deformations in the rod on its overhang in the initial position is shown in fig. 9.

Table 3. Polynomial dependences of the deformations the rod on its overhang and the applied force

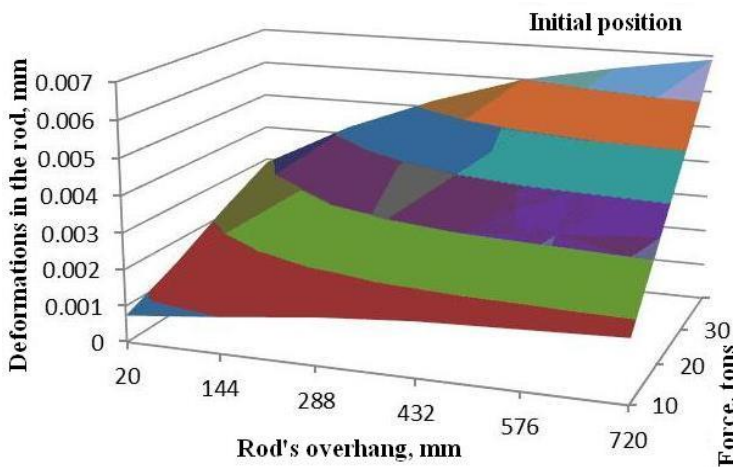| Force, tons	Polynoms	R^2
10	$y = -2E\text{-}09x^2 + 3E\text{-}06x + 0.0007$	0.9981
20	$y = -4E\text{-}09x^2 + 5E\text{-}06x + 0.0013$	0.9965
30	$y = -5E\text{-}09x^2 + 8E\text{-}06x + 0.0021$	0.9999
40	$y = -6E\text{-}09x^2 + 1E\text{-}05x + 0.0028$	0.9984

Fig. 9. The graph of the dependence of the deformations in the rod on its overhang in the initial position

Table 4 shows the polynomial dependences of the rod deformations on its overhang and the applied force. The graph of the dependence of the deformations in the rod on its overhang in the final position is shown in fig. 10.

Table 4. Polynomial dependences of the deformations the rod on its overhang and the applied force

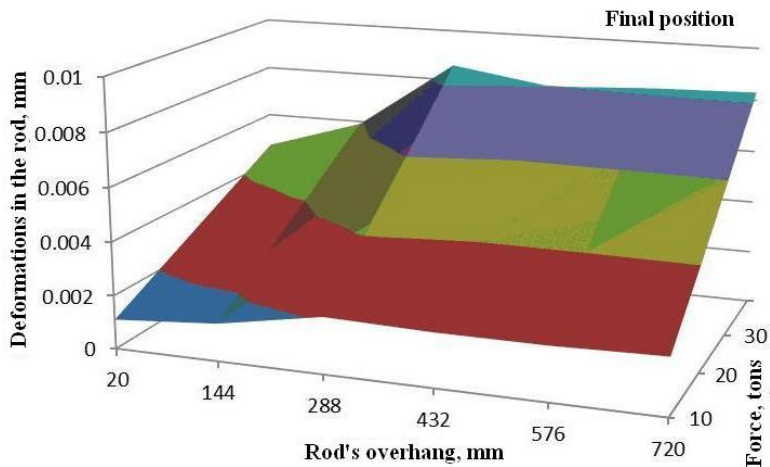| Force, tons	Polynoms	R^2
10	$y = 6E\text{-}12x^3 - 1E\text{-}08x^2 + 6E\text{-}06x + 0.0009$	0.917
20	$y = 1E\text{-}11x^3 - 2E\text{-}08x^2 + 1E\text{-}05x + 0.002$	0.9034
30	$y = 2E\text{-}11x^3 - 3E\text{-}08x^2 + 2E\text{-}05x + 0.003$	0.9128
40	$y = 2E\text{-}11x^3 - 4E\text{-}08x^2 + 2E\text{-}05x + 0.0041$	0.9095

Fig. 10. The graph of the dependence of the deformations in the rod on its overhang in the final position

Table 5 shows the polynomial dependences of the stresses in the hinge on the rod's overhang and the applied force. The graph of the dependence of the stresses in the hinge on the rod's overhang in the initial position is shown in fig. 11.

Table 5. The polynomial dependences of the stresses in the hinge on the rod's overhang and the applied force

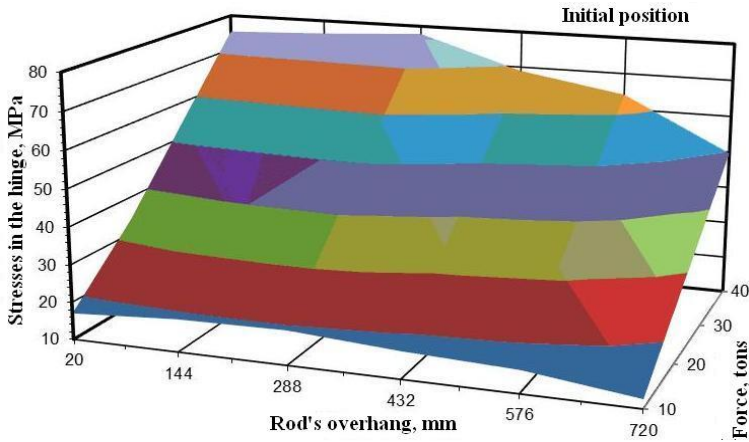| Force, tons	Polynoms	R^2
10	$y = -3E\text{-}05x^2 + 0.0148x + 16.941$	0.975
20	$y = -6E\text{-}05x^2 + 0.0327x + 33.692$	0.961
30	$y = -8E\text{-}05x^2 + 0.0318x + 54.073$	0.9754
40	$y = -9E\text{-}05x^2 + 0.0317x + 74.437$	0.9797

Fig. 11. The graph of the dependence of the stresses in the hinge on the rod's overhang in the initial position

Table 6 shows the polynomial dependences of the stresses in the hinge on the rod overhang and the applied force. The graph of the dependence of the stresses in the hinge on the rod's overhang in the final position is shown in fig. 12.

Table 6. The polynomial dependences of the stresses in the hinge on the rod overhang and the applied force

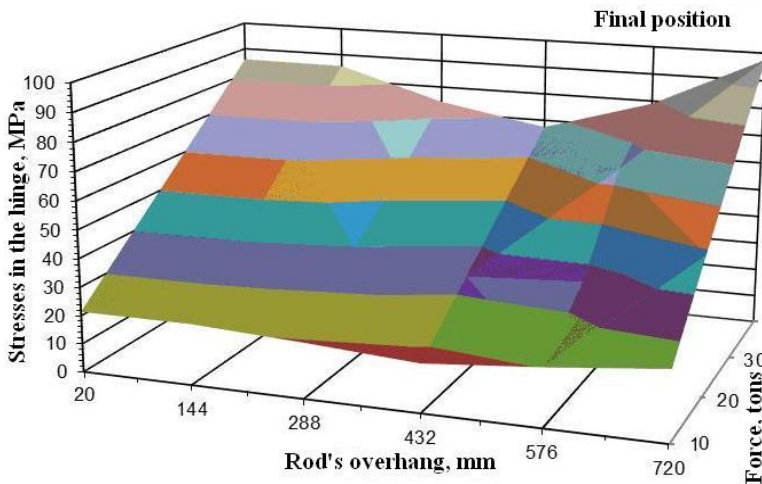| Force, tons	Polynoms	R^2
10	$y = 1E\text{-}07x^3 - 7E\text{-}05x^2 + 0.0049x + 21.529$	0.9137
20	$y = 3E\text{-}07x^3 - 0.0003x^2 + 0.0448x + 41.969$	0.989
30	$y = 2E\text{-}07x^3 - 7E\text{-}05x^2 - 0.0289x + 66.288$	0.8285
40	$y = 4E\text{-}07x^3 - 0.0003x^2 + 0.0041x + 86.959$	0.9488

Fig. 12. The graph of the dependence of the stresses in the hinge on the rod's overhang in the final position

Table 7 shows the polynomial dependences of the deformations in the hinge on the rod overhang and the applied force. The graph of the dependence of the deformations in the hinge on the rod's overhang in the initial position is shown in fig. 13.

Table 7. The polynomial dependences of the deformations in the hinge on the rod overhang and the applied force

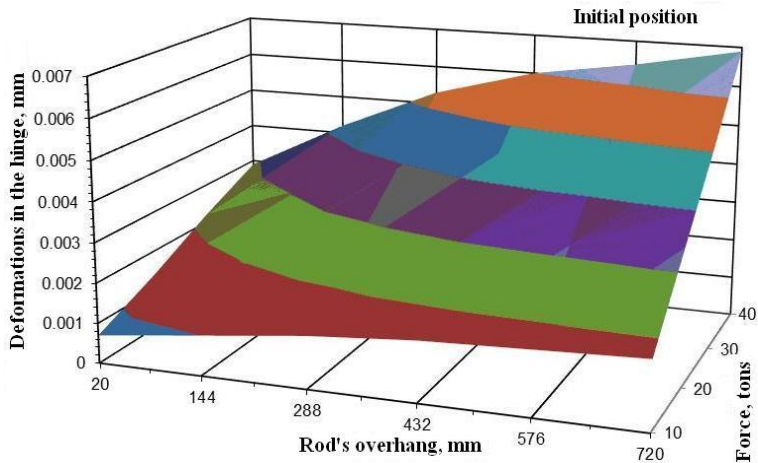| Force, кН	Polynoms	R^2
10	y = -2E-09x^2 + 3E-06x + 0.0006	0.9984
20	y = -4E-09x^2 + 5E-06x + 0.0013	0.9965
30	y = -5E-09x^2 + 8E-06x + 0.0021	0.9986
40	y = -7E-09x^2 + 1E-05x + 0.0028	0.9955

Fig. 13. The graph of the dependence of the deformations in the hinge on the rod's overhang in the initial position

Table 8 shows the polynomial dependences of the deformations in the hinge on the rod overhang and the applied force. The graph of the dependence of the deformations in the hinge on the rod's overhang in the final position is shown in fig. 14.

Table 8. The polynomial dependences of the deformations in the hinge on the rod overhang and the applied force

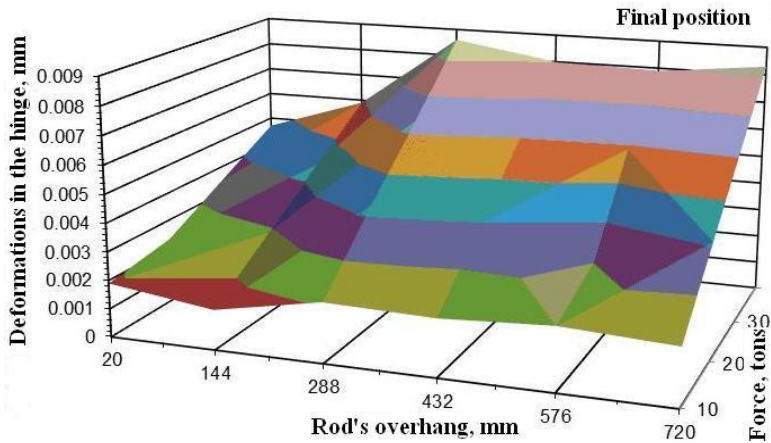| Force, tons	Polynoms	R^2
10	y = -1E-11x^3 + 2E-08x^2 - 4E-06x + 0.0019	0.5811
20	y = 4E-11x^3 - 5E-08x^2 + 2E-05x + 0.0017	0.729
30	y = 2E-11x^3 - 3E-08x^2 + 2E-05x + 0.003	0.9034
40	y = 3E-11x^3 - 5E-08x^2 + 2E-05x + 0.004	0.8989

Fig. 14. The graph of the dependence of the deformations in the hinge on the rod's overhang in the final position

In the process of studying the stress-strain state of the support-guide system with a changing force in the hydraulic cylinder from 10 to 40 tons, stress concentration zones predetermined by design and operational features were identified.

The results obtained allow us to predict the ways to improve the support-guide system as a whole, as well as its individual components.

Conclusion

The obtained results of modeling the support-guide system indicate its non-linearity, i.e. the system is a combination of three elastic elements with a varying of rigidity coefficient. The results can also be used for further detailed modeling in order to develop new technical solutions aimed at improving the operational reliability of horizontal auger-boring complexes when implementing the two-stage technology described above.

The methods used are applicable to the entire adaptable range of structures for boring complexes support-guide systems developed at KuzSTU, with subsequent modeling and analysis after the correction data is entered (depending on the conditions of penetration in specific soil or mining-geological conditions).

References

1. V. Aksenov, V. Sadovets, D. Pashkov, E3S Web of Conf., The 2nd Int. Inn. Min. Symp. (2017)
2. V. Aksenov, A. Efremenkov, V. Sadovets, D. Pashkov, IOP Conf. Ser.: Mat. Sc. And Eng., 012005 (2018)
3. V. Aksenov, V. Sadovets, D. Pashkov, E3S Web of Conf. (2018)
4. B. Danilov, Journ. of Min. Sc., **43** (2007)
5. V. Oparin, B. Danilov, B. Smolyanitski, Journ. of Min. Sc., **46** (2010)
6. B. Danilov, B. Smolyanitski, Journ. of Min. Sc., **49** (2013)
7. A. Gilev, V. Butkin, V. Chesnokov, Rus. Min., 6 (2003)

8. A. Shigin, A. Shigina, A. Gilev, S. Vokhmin, G. Kurchin, Journ. of Theor. and Appl. Inf. Technol, **80**, 1 (2015)

9. R. Muminov, G. Rayhanova, D. Kuziev, Ugol', **5**, 32 (2021)

10. A. Khoreshok, K. Ananiev, A. Ermakov, D. Kuziev, A. Babarykin, Acta Montanistica Slovaca, **25,** 70 (2020)

11. K. Bovin, A. Gilev, A. Shigin, V. Chesnokov, A. Shigina, Journ. of Mech. Eng. and Technol., 10 (2019)

12. R. Kanterman, Fire Eng., **151**, 11 (1998)

13. L. Mametyev, O. Lyubimov, Yu. Drozdenko, 8th Rus.-Chin. Symp. Adv. Eng. Res., **92** (Atlantis Press, 2016)

14. L. Mametyev, O. Lyubimov, Yu. Drozdenko, Journ. of Min. Sc., **53**, 2 (2017)

15. L. Mametyev, O. Lyubimov, Yu. Drozdenko, MATEC Web of Conf., **297**, 03003 (2019)

16. Pat. 165050 of Russian Federation (2016)

17. Pat. 190838 of Russian Federation (2019)

18. Pat. 198342 of Russian Federation (2020)